OSCILLATIONS OF AIR CUSHION VEHICLES

by

Robert E. Butler

A Thesis Submitted to the Faculty of the

DEPARTMENT OF MECHANICAL ENGINEERING

In Partial Fulfillment of the Requirements
For the Degree of

MASTER OF SCIENCE

In the Graduate College

THE UNIVERSITY OF ARIZONA

1961

STATEMENT BY AUTHOR

This thesis has been submitted in partial fulfillment of requirements for an advanced degree at The University of Arizona and is deposited in The University Library to be made available to borrowers under rules of the Library.

Brief quotations from this thesis are allowable without special permission, provided that accurate acknowledgment of source is made. Requests for permission for extended quotation from or reproduction of this manuscript in whole or in part may be granted by the head of the major department or the Dean of the Graduate College when in their judgment the proposed use of the material is in the interests of scholarship. In all other instances, however, permission must be obtained from the author.

SIGNED: Robert L. Butler

APPROVAL BY THESIS DIRECTOR

This thesis has been approved on the date shown below:

Willard L. Rogers
W. L. ROGERS

May 8, 1961
Date

Professor of Mechanical Engineering

ABSTRACT

The main purpose of this thesis was to determine if self-excited oscillations are possible in plenum chamber air cushion vehicles.

A literature search was conducted to determine what work had been accomplished to date. Theoretical predictions were made from an analysis of a mathematical model.

Experimental tests were conducted to verify the theoretical predictions.

Conclusions were drawn from a comparison of the theoretical and experimental work in this thesis.

ACKNOWLEDGEMENTS

I would like to express my sincere thanks and gratitude to Dr. W. L. Rogers for his invaluable assistance in conducting this study and his constructive advice and suggestions during the preparation of the manuscript.

I am also deeply indebted to F. L. Cummings for his help and advice in use of laboratory apparatus.

Graduate study at the University of Arizona was made possible by the U. S. Army. For this opportunity, I am indeed grateful.

To all others who helped in any way and are not mentioned here, I am sincerely grateful.

TABLE OF CONTENTS

CHAPTER PAGE

PREFACE

The progress made in air travel during the last twenty years has been enormous, but lesser progress seems to have been made in increasing the rapidity of travel on land or over water.

The air cushion vehicle, or ground effect machine as it is often called, is a new and unique way of surface travel. The air cushion vehicle uses no wheels and it can be used over water as well as over land. The vehicle's engine drives an impeller that compresses the air inside and under the vehicle. The pressure of the air lifts the vehicle off the surface over which it is traveling. Since there is very little friction between the vehicle and the ground, the air cushion vehicle can be moved easily in any horizontal direction by a small force.

The ability to travel over muddy and marshy terrain, and to traverse terrain which has few if any improved road nets, makes the air cushion vehicle particularly valuable in military logistical operations.

At present, studies are being made to determine the feasibility of the air cushion vehicle for many different uses. One of the more spectacular achievements resulting

from these studies was the crossing of the English Channel on July 25, 1959, by the SR-N1, an air cushion vehicle weighing 8,500 pounds.[1*]

While most of the present work on the ground effect machines is being done on the annular jet type vehicle, the extreme simplicity of the plenum chamber air cushion vehicle makes it very attractive. The plenum chamber type vehicle is the subject of the theoretical and experimental work described in this thesis. The specific purpose of this thesis is to study the motion of a hovering plenum chamber air cushion vehicle which has been disturbed from an altitude equilibrium position, and particularly to determine whether self-excited vertical oscillations are possible. A circular planform is assumed throughout.

* Refers to List of References.

CHAPTER I

BACKGROUND AND THEORY

1.1 Introduction - The two basic forms of the air cushion vehicle are the annular jet type and the plenum chamber type. Both types are called Ground Effect Machines (GEM) because they utilize a cushion of low pressure air between the vehicle and the ground to obtain lift in excess of the basic momentum change usually associated with air-moving lifting systems. Figures 1.1 and 1.2 show these low pressure regions for both types of vehicles. The annular jet confines a bubble of low pressure air beneath the base of the vehicle by means of a jet of air exhausted around the periphery of the vehicle. The plenum chamber maintains the low pressure air within the body itself. This air is allowed to leak out around the periphery of the vehicle. When the flow into either vehicle is equal to the flow out around the periphery the vehicle will hover at an altitude equilibrium height.

A search of the literature pertaining to air cushion vehicles reveals that most of the work to date has been done on the annular jet type rather than on the plenum chamber type. While it is thought that the annular jet vehicle is

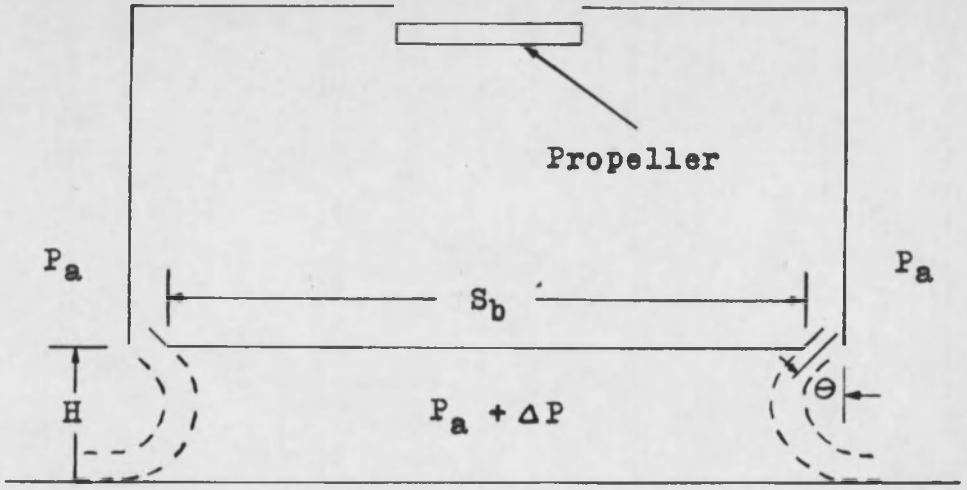

Figure 1.1

Region of low pressure air cushion for annular jet

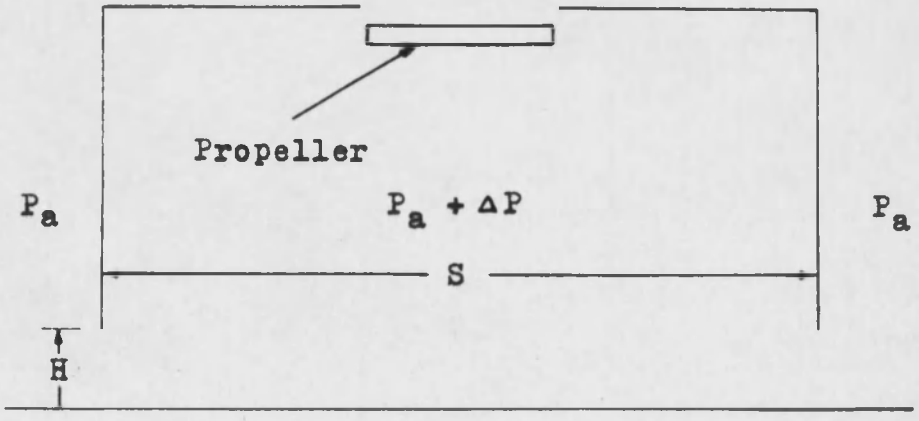

Figure 1.2

Region of low pressure air cushion for plenum chamber

more adaptable to commercial use, it is too early to conclude that the annular jet inherently enjoys a performance advantage over the plenum chamber vehicle because the plenum chamber vehicle has not received the same amount of attention as the annular jet.[2]

1.2 Existing theory and experimental data for plenum chamber air cushion vehicles- While the plenum chamber vehicle is endowed with structural simplicity, the internal flow and performance characteristics are far from simple. An example of the complexity of internal flow is indicated by the existence of negative lifting pressure at comparatively low height-to-vehicle diameter ratios (h/D)[3] under certain conditions. The performance characteristics are more difficult to describe for the "simple" GEM than for conventional aircraft since plenum chamber pressure and altitude have first order effects in addition to the first order effects due to velocity and attitude found in conventional aircraft.[4]

The original work done in power estimation for plenum chambers was based on the assumption that the velocities in the plenum chamber are low enough so that the lift on the vehicle is due only to plenum chamber static pressure.[5] This assumption is true only for low h/D's. More recent theories for the plenum chamber assume that the lift on the vehicle is due to the static pressure within the chamber and momentum thrust. However, for h/D below 0.10 it has been

found that test results, for plenum chambers with the flow attached to the wall, correlate with theoretical predictions which assume that the lift on the vehicle is due only to plenum chamber static pressure.[6]

The state of the art has progressed to the point where stability tests are being conducted for air cushion vehicles. While much more work will be required in the field, certain characteristics have been indicated. Free hover flights of plenum chamber models have indicated static instability in pitch and roll for h/D above about 0.03.[7] In the model in reference 7, the flow was attached to the wall. The reason for this static instability is apparently due to momentum thrust at the periphery of the vehicle. Since the flow is attached to the wall, the flow at the exit has a vertical component. When the model is tilted, the vertical velocity decreases at the side closest to the ground. This decrease in velocity will decrease the momentum thrust at this edge of the vehicle. The change of the moment about the center of gravity of the vehicle due to this decrease in momentum thrust will be destabilizing.

In other experimental tests it has been determined that the static pressure within the plenum chamber varies inversely with a function of the square of the height as compared with the inverse linear variation of the annular jet.[8] The static pressure is also a function of the fourth power of the ratio of the fan diameter to the overall plenum

chamber diameter.

Other experiments showed that when the discharge area is greater than the fan area, the discharging jet is not capable of maintaining a seal between the plenum chamber and the atmosphere.[9] Under such conditions, the plenum chamber is said to be vented to the atmosphere. Figure 1.3 shows a characteristic flow pattern of the air in the plenum chamber. When the chamber is vented to the atmosphere, the total pressure within the chamber approaches atmospheric pressure and the static pressure within the chamber must be below atmospheric pressure due to the high velocity recirculating air. A negative lift is produced since the static pressure on the inside walls of the plenum chamber is less than the atmospheric pressure on the outside walls of the chamber. As the height of the vehicle increases, the recirculation decreases. At $h/D = 1$, there is very little circulation and the flow of air approaches a jet flow.

Free hover stability tests have shown that strong vertical pulsing can take place at certain h/D's.[10] This vertical oscillation is the primary subject of this thesis.

1.3 Theoretical model and assumptions - Figure 1.4 shows the system under consideration. It includes the plenum chamber, the fan system, the air within the chamber, and the air in the volume beneath the planform area, S.

The following assumptions are used in the theoretical study of the model:

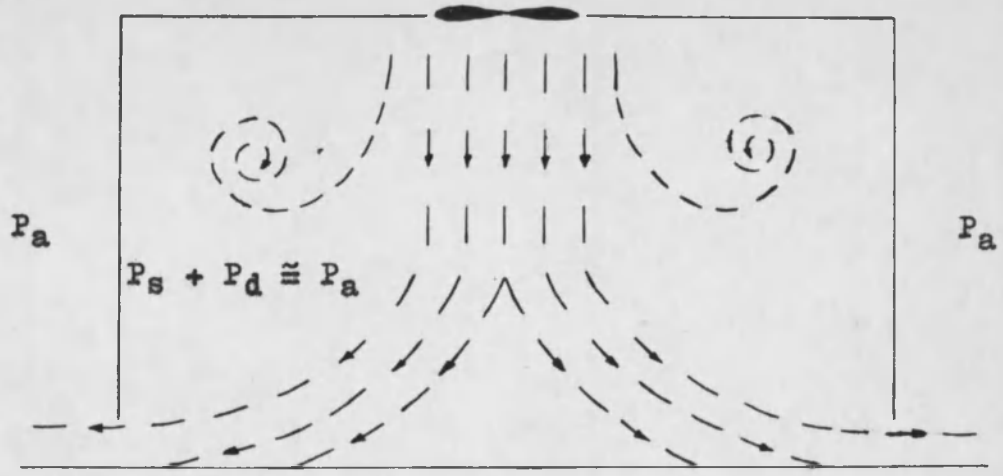

Figure 1.3

Characteristic air flow pattern for plenum chamber vented to atmosphere

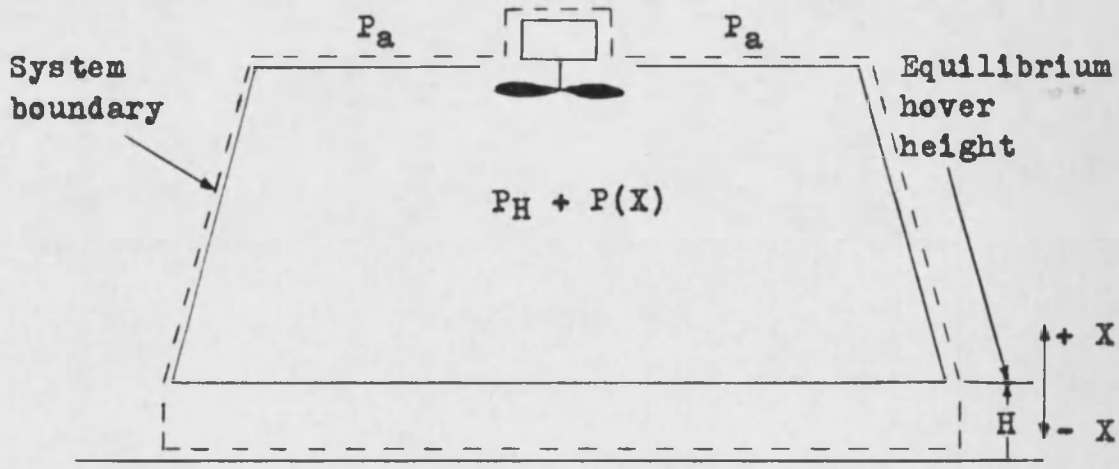

Figure 1.4

Model system and sign convention for displacement

a) The mass rate of inflow of air into the system is constant for small displacements from equilibrium hover position.

b) The lift on the model is due to static pressure only at low h/D's. (Other experiments have shown that the exit jet velocity in the X direction of the air from the plenum chamber is sufficiently low at these h/D's to justify this assumption.)

c) The mass of air in the system is much smaller than the mass of the hardware of the system.

d) The air in the system is in local thermodynamic equilibrium at all times.

e) The compression of the air in the system due to the vertical oscillation of the vehicle follows an isentropic process.

f) Viscous damping is assumed, and the damping coefficient, c, is assumed to be linear for small displacements from the equilibrium hover position.

1.4 Qualitative analysis of mass flow in system during displacement from equilibrium hover position - The continuity consideration yields the change of mass per unit time, $\dot{m}$. For the equilibrium height, H, $\dot{m} = o$. If the equilibrium hover height is chosen as the zero datum plane and displacement, X, in the upward direction is positive, then $\dot{m}$ will be positive for negative values of X and negative for positive values of X. Figure 1.3 illustrates this

convention.

1.5 Equation of motion of theoretical model - The equation of motion for the plenum chamber can be written by consideration of the forces on the chamber shown in the free body diagram of Figure 1.5

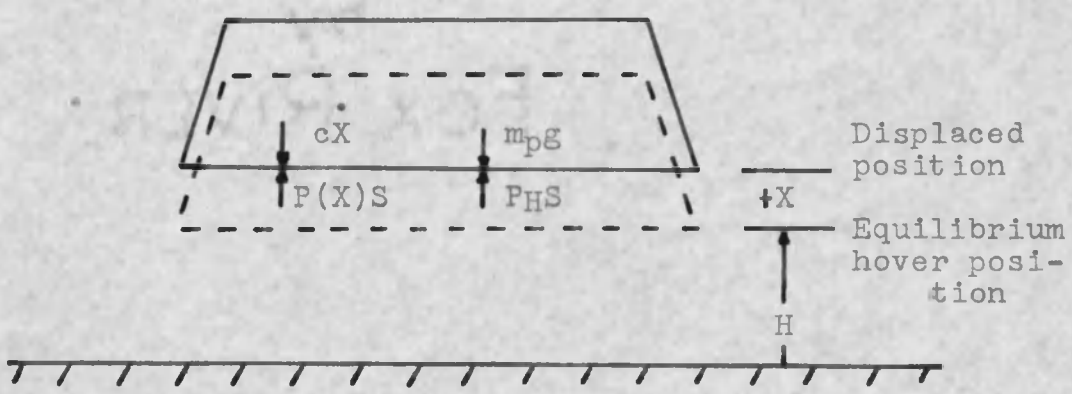

Figure 1.5 Free body diagram of theoretical model.

$$m_p\ddot{X} = -c\dot{X} + P_HS + P(X)S - m_pg \qquad (1.1)$$

P(X) is the gage pressure above or below the gage pressure within the plenum chamber at equilibrium hover position, P_H, expressed as a function of the displacement, X. The constant forces m_pg and P_HS are equal and opposite and counteract each other.

A second equation relating P(X) and X can be obtained from the gas law expressed by

$$(P_x + P_H + P_a)V_x = m_xRT_x \qquad (1.2)$$

where P_x is P(X) as defined above, P_a is atmospheric pressure,

and $V_X = V_H + XS$. Differentiation with respect to time, and remembering that P_H is constant, yields

$$\dot{P}(X) = m_X R V_X^{-1})\dot{T} + (RT_X V_X^{-1})\dot{m}(X) - (m_X R T_X V_X^{-2})\dot{V}_X \qquad (1.3)$$

The compression of the mass of air within the chamber itself is assumed to be adiabatic and reversible. This condition permits the use of the isentropic relation

$$T_X V_X^{k-1} = \text{constant} \qquad (1.4)$$

which can be differentiated to yield $\dot{T}$ as a function of $\dot{V}_X$.

$$\dot{T} = T_X V_X^{-1}(1-k)\dot{V}_X \qquad (1.5)$$

Combining the above equations, we get

$$\dot{P}(X) = (-km_X R T_X V_X^{-2})\dot{V}_X + (RT_X V_X^{-1})\dot{m}(X) \qquad (1.6)$$

The volume of the system can be expressed by

$$V_X = V_H + SX \qquad (1.7)$$

and the rate of change of volume with respect to time is

$$\dot{V}_X = S\dot{X} \qquad (1.8)$$

Substituting the result from 1.8 into 1.6, the expression for the rate of change of pressure becomes

$$\dot{P}(X) = (-km_X R T_X V_X^{-2} S)\dot{X} + (RT_X V_X^{-1})\dot{m}(X) \qquad (1.9)$$

The coefficient of $\dot{X}$ represents the change of pressure within the plenum chamber due to a change in volume of the system and the coefficient of $\dot{m}(X)$ represents the change of pressure within the plenum chamber due to the change in mass of the system.

Differentiating 1.1 with respect to time and substituting 1.9 for $\dot{P}(X)$, the following equation results

$$\dddot{X} + \frac{c}{m_p}\ddot{X} + \frac{(km_x RT_x V_x^{-2} S^2)}{m_p}\dot{X} - \frac{(RT_x V_x^{-1} S)}{m_p}\dot{m}(X) = 0 \qquad (1.10)$$

This equation describes the dynamic behavior of the model system.

For use in qualitative stability analysis of equation 1.10, $\dot{m}$ will now be expressed as a function of X. Since $\dot{m}(X)$ is the rate of mass accumulation in the system, we can say

$$\dot{m}(X) = \rho_1 v_1 A_1 - (\rho_x v_e \pi d)H - (\rho_x v_e \pi d)X \qquad (1.11)$$

where $\rho_1 v_1 A_1$ is the constant mass inflow rate and $(\rho_x v_e \pi d)H + (\rho_x v_e \pi d)X$ is the mass outflow rate. At hover height, H,

$$\rho_1 v_1 A_1 = \rho_H v_H \pi dH \qquad (1.12)$$

For very small displacements from the hover position, ρ_h and v_H change slightly to become ρ_x and v_e as shown in equation 1.11. As a first approximation, these changes can

be considered negligible, and equation 1.11 reduces to the linear form

$$\dot{m}(X) = -(\rho_x v_e \pi d)X \tag{1.13}$$

Using this result in equation 1.10 and substituting $(P_x+P_H+P_a) = \rho_x RT_x$, the equation of motion of the model for small displacements about the equilibrium hover position becomes

$$\dddot{X} + \frac{c}{m_p}\ddot{X} + \frac{k(P_x+P_H+P_a)V_x^{-1}S^2}{m_p}\dot{X} + \frac{(P_x+P_H+P_a)V_x^{-1}v_e\pi dS}{m_p}X = 0 \tag{1.14}$$

1.6 Theoretical stability analysis and predictions - Inspection of equation 1.14 shows that it is linear, allowing use of the Routh criterion for a qualitative analysis for stability.

For a cubic linear differential equation such as

$$\dddot{X} + A_2\ddot{X} + A_1\dot{X} + A_0X = 0 \tag{1.15}$$

which has the characteristic equation

$$S^3 + A_2S^2 + A_1S + A_0 = 0 \tag{1.16}$$

the complete criterion for stability, according to Routh, is that all coefficients, A, are positive and that $A_1A_2 > A_0$.[11]

Since all of the signs of the coefficients are positive, the only additional requirement for stability is $A_1A_2 > A_0$. This condition requires that

$$\frac{k(P_x + P_H + P_a)V_x^{-1}S^2c}{m_p} > \frac{(P_x + P_H + P_a)V_x^{-1}v_e\pi dS}{m_p} \qquad (1.17)$$

which reduces to

$$\frac{kcd}{4m_p} > v_e \qquad (1.18)$$

From the model to be tested, d = 1.3 ft., m_p = 0.21 slug. The specific heat ratio, k, is assumed to be 1.4. To estimate v_e, the equation

$$v_e = \left(\frac{2P_x}{\rho_x}\right)^{\frac{1}{2}} \qquad (1.19)$$

will be used. For P_x = 1 inch of water, and ρ_x = 0.0023, v_e = 67 ft/sec. (The validity of assuming the static pressure is approximately 1 inch of water will be shown in the experimental portion of this thesis.) For the system to be stable, the damping coefficient, c, must be greater than about 31 lb_f sec/ft. It is reasonable to assume that the actual c is far less than this value for the model tested, and therefore the system is unstable.

From the interpretation in section 1.4 of $\dot{m}$ as a function of displacement, and the change of the lifting pressure within the chamber due to change in volume of the system, the phase angle between the lifting pressure within the plenum chamber and displacement should be approximately 90°.

From the preceding analyses, it can be concluded:

a) The vehicle should oscillate once it is disturbed from the equilibrium hover position.

b) The phase angle between the plenum chamber lifting pressure and displacement should be approximately 90°.

c) Stability is promoted by small exit velocity v_e and large size to weight ratio $\frac{d}{m_p}$ as well as by a large damping coefficient c.

CHAPTER II

TEST MODELS

2.1 Small plenum chamber model - The small plenum chamber was made from a round dish pan. Figure 2.1a is a photograph of the model as it looked after it was instrumented for tests. Figure 2.2 shows the dimensions of the model and the location of the six pressure taps used during the tests. Set screws, which permitted the model to be supported at heights up to about two inches, are also shown in Figure 2.2.

An electric motor was used as the power source for the model. The motor was rated one-seventh horsepower and the rated speed of the motor was 10,000 rpm. The speed of the motor was controlled by a variac. A model airplane propeller was used for the fan blade. The propeller was originally a 12-6 propeller, meaning that the propeller was twelve inches in diameter and the pitch (6) was such that the propeller would theoretically travel six inches forward for each revolution. Due to the size of the model, the propeller was cut down to eight inches in length. The propeller protruded one fourth inch into the plenum chamber as shown in Figure 2.2.

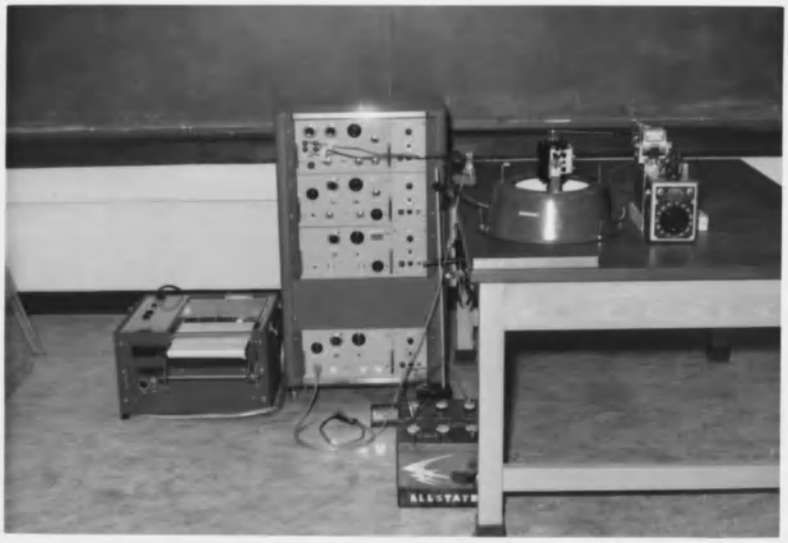

Figure 2.1a

Small plenum chamber model and test apparatus

Figure 2.1b

Large plenum chamber model

Scale 1:2.8 (Approximate)

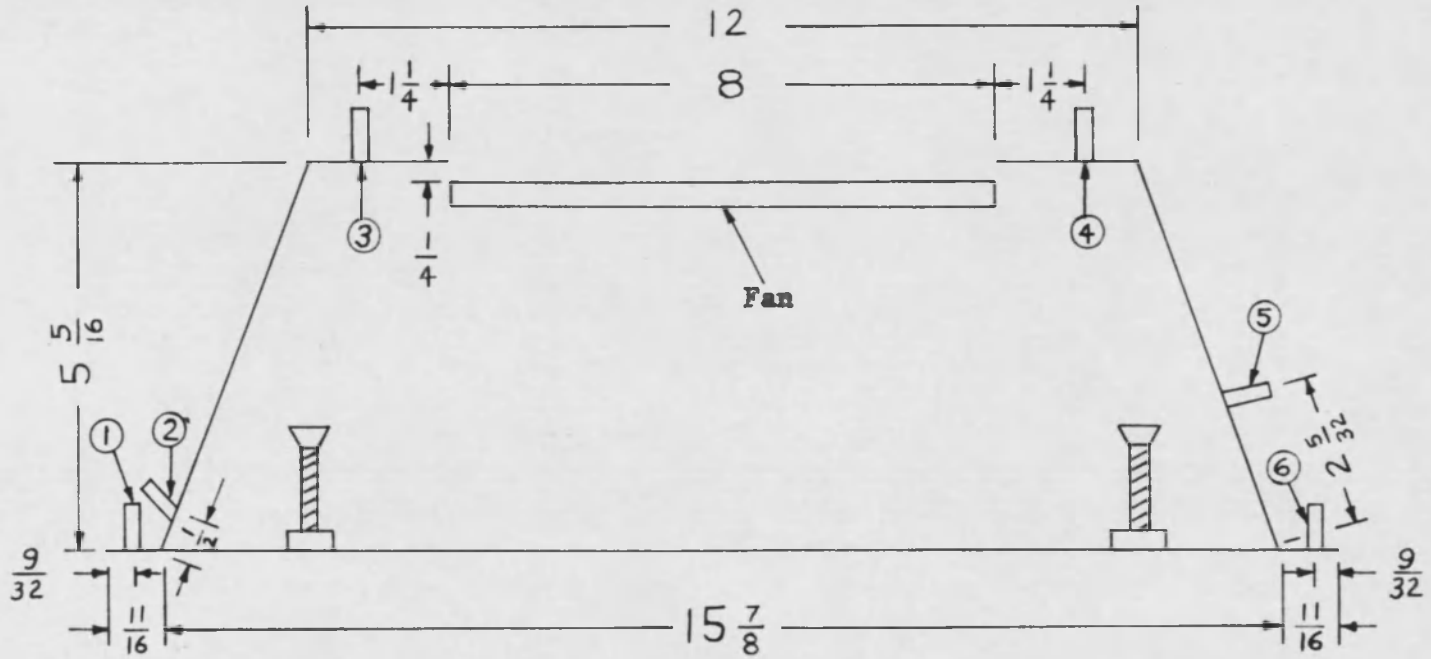

Figure 2.2

Small plenum chamber model dimensions

and location of pressure taps

2.2 Large plenum chamber model - The large plenum chamber model was made from a round tub. Figure 2.1b is a photograph of the model as it looked during testing. Copper plates were soldered to the inside of the tub to provide surfaces to accommodate fourteen pressure taps. Two other taps were located on the lip of the periphery of the model. Locations of these pressure taps are shown in Figure 2.3. Four metal rods were attached to the top of the model in order that the weight of the model could be counterbalanced to change the weight which had to be lifted during hovering.

The same fan system that was used for the small plenum chamber was used for the large plenum chamber.

Scale 1:4 (Approximate)

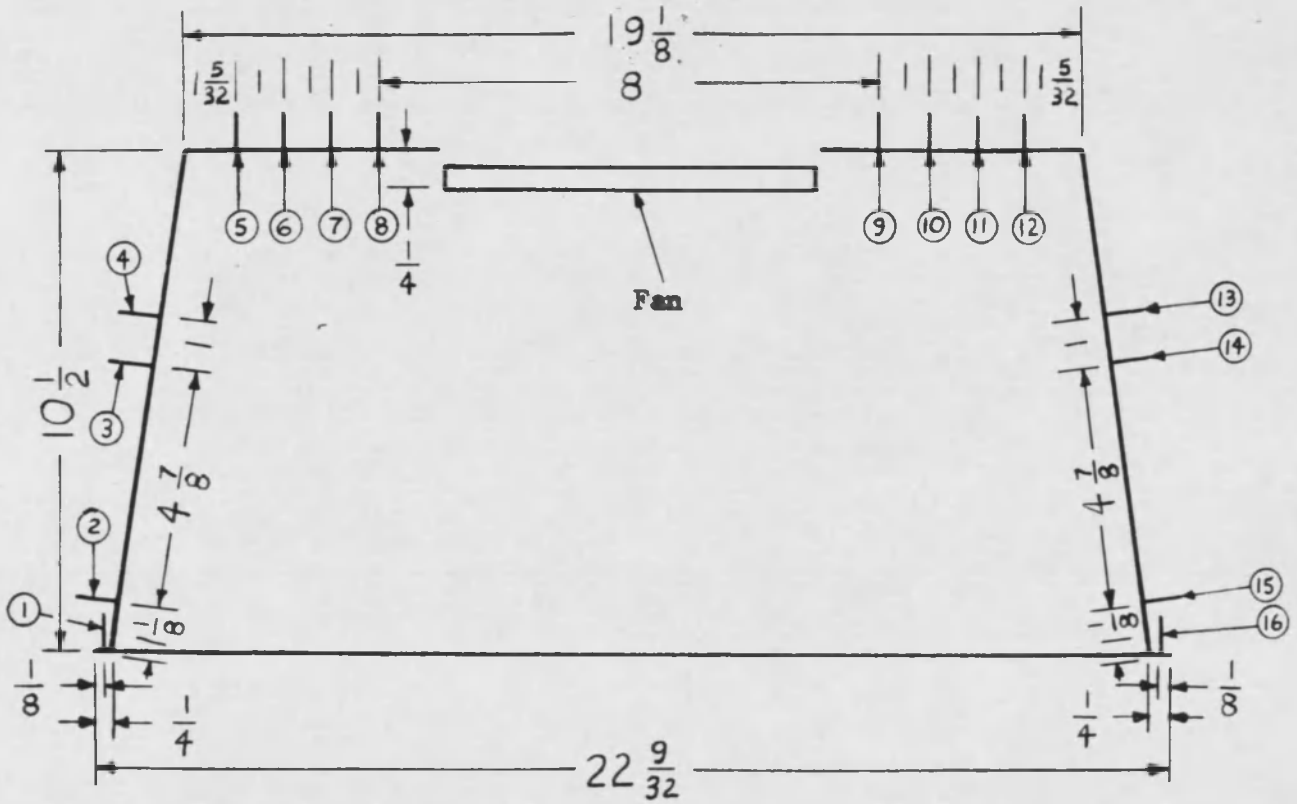

Figure 2.3

Large plenum chamber model dimensions

and location of pressure taps

CHAPTER III

EXPERIMENTAL PROCEDURE

3.1 Self-excited vertical oscillations - The primary subject of this thesis is the study of the motion of a hovering plenum chamber air cushion vehicle which has been disturbed from its equilibrium position. The experimental testing of the small plenum chamber to verify the theoretical predictions of Chapter I consisted of the following two tests:

a) Observation of the motion of the vehicle when disturbed.

b) Determination of the phase angle between the plenum chamber pressure and the displacement.

The first part of the first test was accomplished by permitting the plenum chamber to attain its hovering height with maximum voltage rating applied to the fan motor. The power input at this hovering height was 318 watts. All motion of the vehicle was stopped by steadying the vehicle by hand after it reached its maximum height. Then the model was displaced in a negative (downward) direction and the motion of the model was observed. At this same height, the model was observed when no external

disturbing force was placed on the model. For all free hover testing, the model was restrained from rotating or traversing by two strings attached to the periphery of the model.

For the second part of the first test, the power to the fan motor was adjusted to 170 watts by using the variac. At this power the model hovered at a height just off the table. As in the first part of the test, all motion of the model was stopped by steadying the model by hand. The model was observed while hovering at this height when no external disturbing force was applied and the motion was observed when a disturbing external force was applied.

The last part of the first test was conducted by adjusting the power to the fan motor to two values, 300 watts and 230 watts, between the extreme values used in parts one and two. Again the model was steadied by hand and the motion of the model was observed.

The second test was conducted to determine if a phase angle between the plenum chamber lifting pressure and the displacement could be observed. A schematic diagram of the test apparatus used in this test is shown in Figure 3.1. Figure 2.1a is a photograph of the model and other apparatus in position for the test.

The pressure variations with time were measured by a Statham temperature compensated pressure transducer which utilizes strain sensitive resistance wires arranged in the

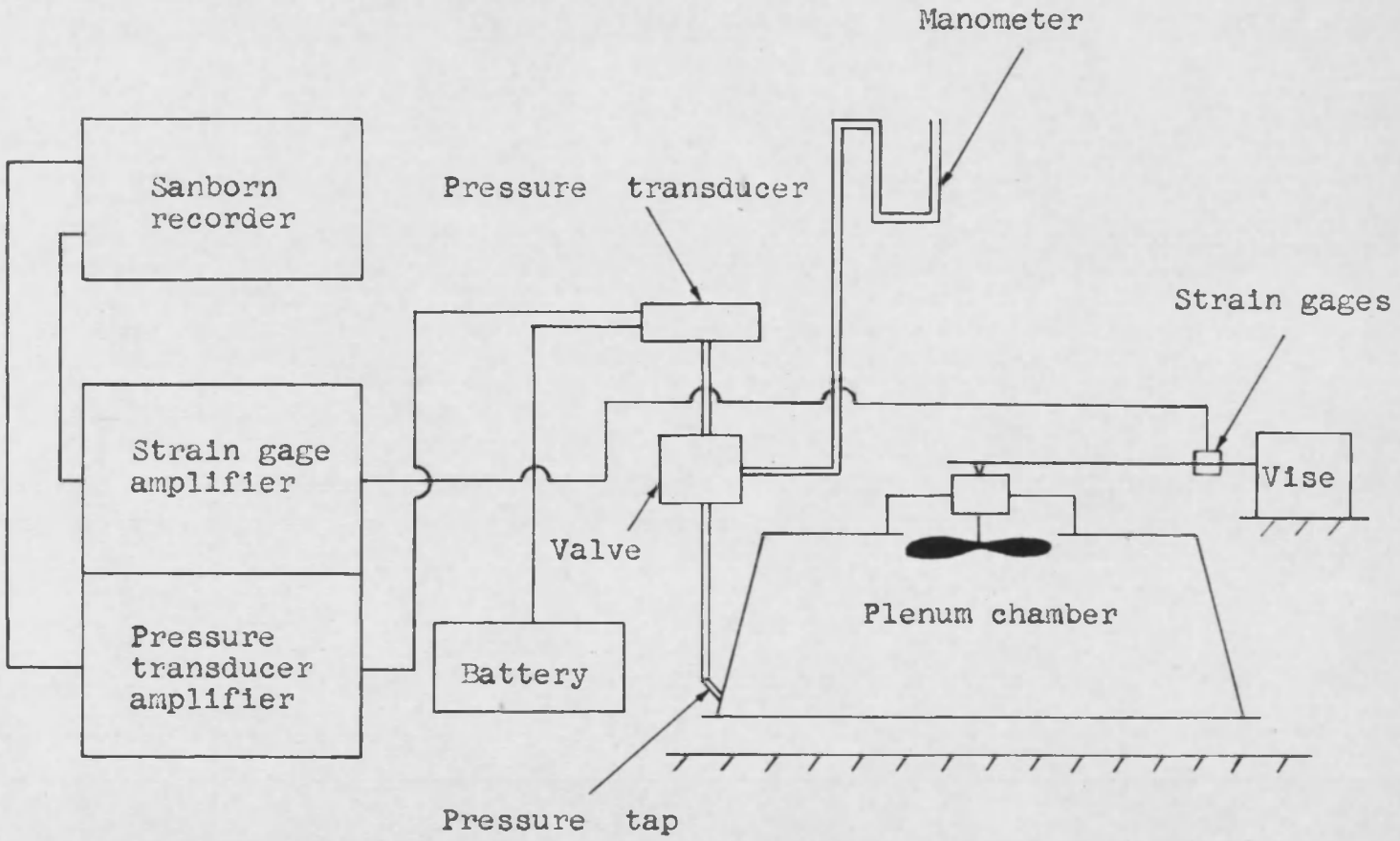

Figure 3.1

Diagram of experimental apparatus

form of a Wheatstone bridge to detect pressure changes. The compensated temperature interval is - 65°F to + 250°F. The pressure range of the transducer is ± 1 psi. This pressure transducer was connected to the pressure tap on the model by a short one-quarter inch rubber hose. The lifting pressure within the chamber, as sensed by the pressure transducer, was recorded as a function of time on a multiple channel Sanborn recorder.

The displacement, with respect to time, of the model was measured by two strain gauges mounted on a thin flexible bar. This bar was clamped in a heavy vise, thus forming a cantilever beam. A stud on the bar was positioned on top of the motor so that a vertical movement of the plenum chamber would cause a deflection of the bar. This deflection of the bar caused the vertical motion of the model to be sensed by the strain gauges. A low level pre-amplifier and the same recorder used to measure the pressure variations were used to record the vertical displacement of the model. A small external force was placed on the model by the cantilever beam, but it is felt that this force was sufficiently small for the small deflections involved that the only effect it had on the system was to act as a very weak spring force.

The lifting pressure variations and the displacement were recorded simultaneously on the multiple channel Sanborn recorder. Examination of the recording permitted a

qualitative measurement of the phase angle between lifting pressure in the plenum chamber and the displacement.

A third test was conducted to determine the frequency of oscillation at different power inputs to the fan motor. This test consisted of recording the static pressure variations, from pressure tap number three, on the model, at different power inputs to the fan motor. The frequency of oscillation was obtained by counting the number of cycles for 3-6 seconds and dividing by the time on the Sanborn recording.

3.2 Plenum chamber lifting pressure as a function of h/D - In order to determine the plenum chamber lifting pressure as a function of h/D, the small model was supported solidly at heights varying from 0 to $1\frac{13}{16}$ inches by three set screws, and the plenum chamber static pressure was measured at each height. A 36 inch water manometer, with one leg connected to pressure tap number three on the model by a three foot length of one-quarter inch rubber hose and with the other leg vented to the atmosphere, was used to obtain the gauge value of the static pressure within the plenum chamber. The reading on each leg of the manometer was taken at the mid-point of the small random fluctuations which were present. Each reading was recorded to the nearest 0.025 inch.

3.3 Negative lift characteristic - The lift on the model, as a function of h/D, was measured to compare the

negative lift characteristic of the small model used in the experimental portion of this thesis with the negative lift characteristic reported by other authors. The plenum chamber was supported by a spring balance attached to the motor housing by a small wire sling. A constant voltage input to the fan motor was used throughout the test. The model was raised to nine different heights by exerting a force on the spring balance. The spring balance was read for each height. The height was read to the closest 1/32 inch and the spring balance was read to the closest 1/4 pound.

3.4 Pressure distribution in large plenum chamber - In order to determine a qualitative analysis of the pressure distribution within the plenum chamber, the large model was "flown" at three different heights. Due to the weight of the model and the limited capacity of the fan, the model had to be counterbalanced with external weights before it would hover at other than very low h/D's. The pressure taps on the plenum chamber were connected to a multiple manometer which permitted the pressure within the chamber to be visualized for the different heights.

CHAPTER IV

RESULTS AND CONCLUSIONS

4.1 Comparison of theoretical stability predictions and experimental results - The small plenum chamber oscillated with self-excited oscillations as predicted in Chapter I. At h/D's between 0.006 and 0.009, the highest attainable h/D with the fan system used, the model oscillated vertically in a violent manner.

According to equation 1.14, the amplitude of the oscillation should increase to infinity. For h/D's greater than 0.006, the small plenum chamber was observed to oscillate with an increasing amplitude until it came into contact with the surface over which it was "flying". After coming into contact with this surface, the model continued to oscillate with constant amplitude.

To test for static stability at the highest attainable h/D the model was tilted in roll and pitch. The model responded with vertical oscillations only, which indicated static stability. The model also exhibited static stability at very low h/D's. Since the tests on the model indicated static stability at the lowest and highest h/D's, the model was apparently statically stable in the regime where the

tests were conducted. This result was expected since the model was operating at h/D's where the velocity of the air leaving the chamber in the X direction is assumed to be sufficiently low so the lift due to momentum thrust is negligible.

In the regime of h/D's below about 0.006 the small model was found to be statically and dynamically stable. Since the main subject of this thesis is regimes of instability due to self-excited oscillations, the study of the observed stable regime is limited to a possible explanation as follows.

If, for all values of small displacements X, $\dot{m}$ becomes essentially independent of X and approaches zero, equation 1.10 can be reduced to

$$m_p\ddot{X} + c\dot{X} + (km_x RT_x V_x^{-2} S^2)X + C = 0 \qquad (4.1)$$

The constant force, C, arises from the integration of equation 1.10 and can be shown to be zero by inspection of the forces on the system in Figure 1.5. This form of equation 1.10 represents a stable system.

An analysis of the system gives a qualitative picture of $\dot{m}$. At zero hover height, equilibrium hover height and a height where the model is out of ground effect, $\dot{m} = 0$. In addition, $\dot{m}$ is independent of X out of ground effect. It is thought that it is possible that $\dot{m}$ can be independent of X for very low hover heights also. For

this condition, equation 4.1 is the equation of motion.

The large plenum chamber model had the same general characteristics as those shown by the small model. No attempt was made to determine scaling effects because the models were not geometrically similar.

Theoretical predictions in Chapter I show that the phase angle between the static pressure in the plenum chamber and the displacement should be approximately 90°. Figure 4.1, made by the multiple channel Sanborn recorder, shows the simultaneous changes in displacement and pressure with respect to time. The record was obtained from a test on the small plenum chamber model. The displacement and static pressure are shown to be approximately 90° out of phase as predicted.

4.2 Discussion of other experimental observations- Figure 4.2 shows frequency of oscillation of the small plenum chamber model in free hover as a function of power input to the fan motor. Since the theoretical analysis was performed primarily to predict instability, no theoretical numerical values of frequency were predicted. The larger volume of the system at the higher fan powers would be expected to decrease the frequency. The experimental curve shows this.

Lift on the small plenum chamber, when supported at various heights, is shown in Figures 4.3 and 4.4 as a function of h/D. At h/D's greater than about 0.03 the static

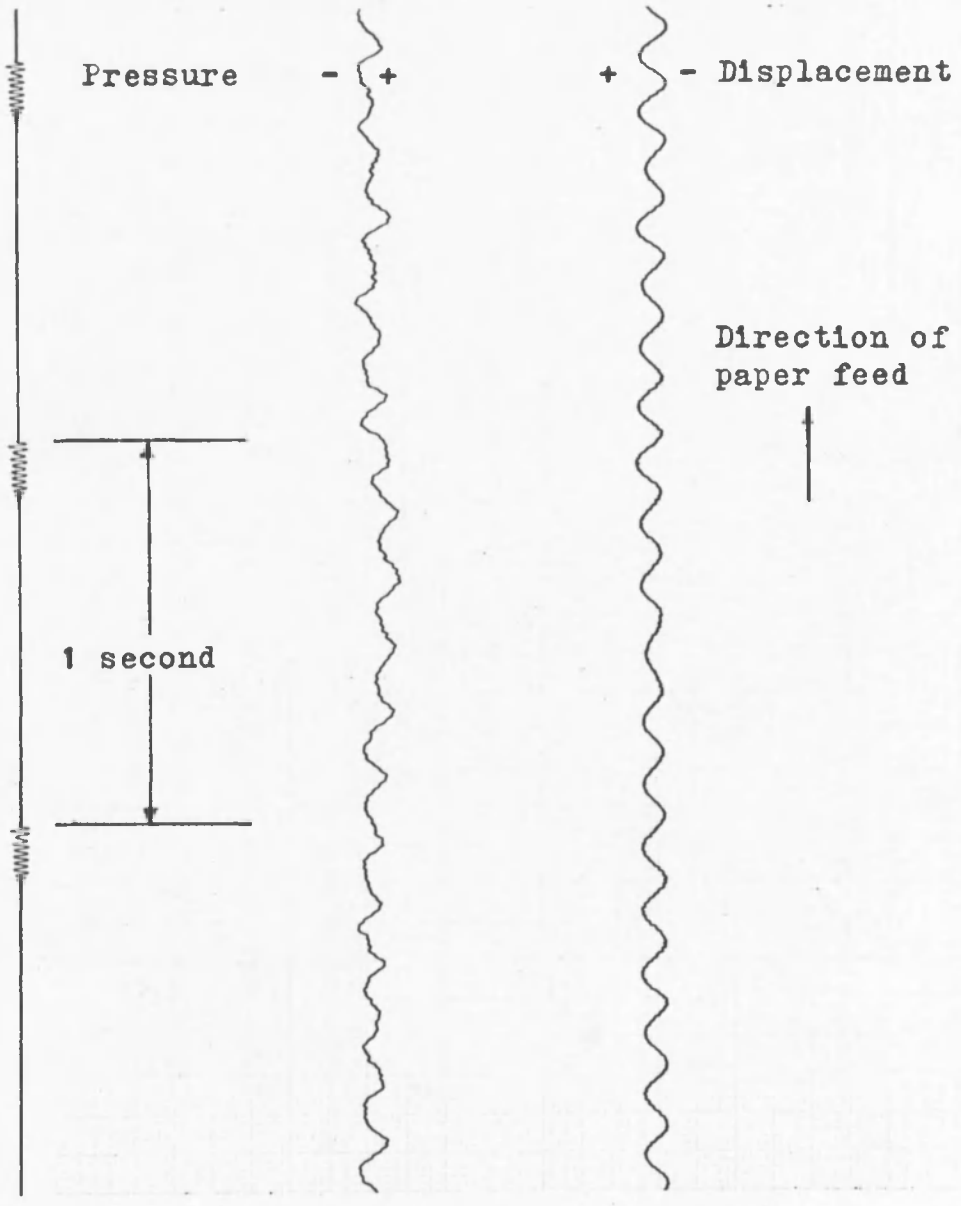

Figure 4.1
Variation of pressure and displacement
in small plenum chamber with time

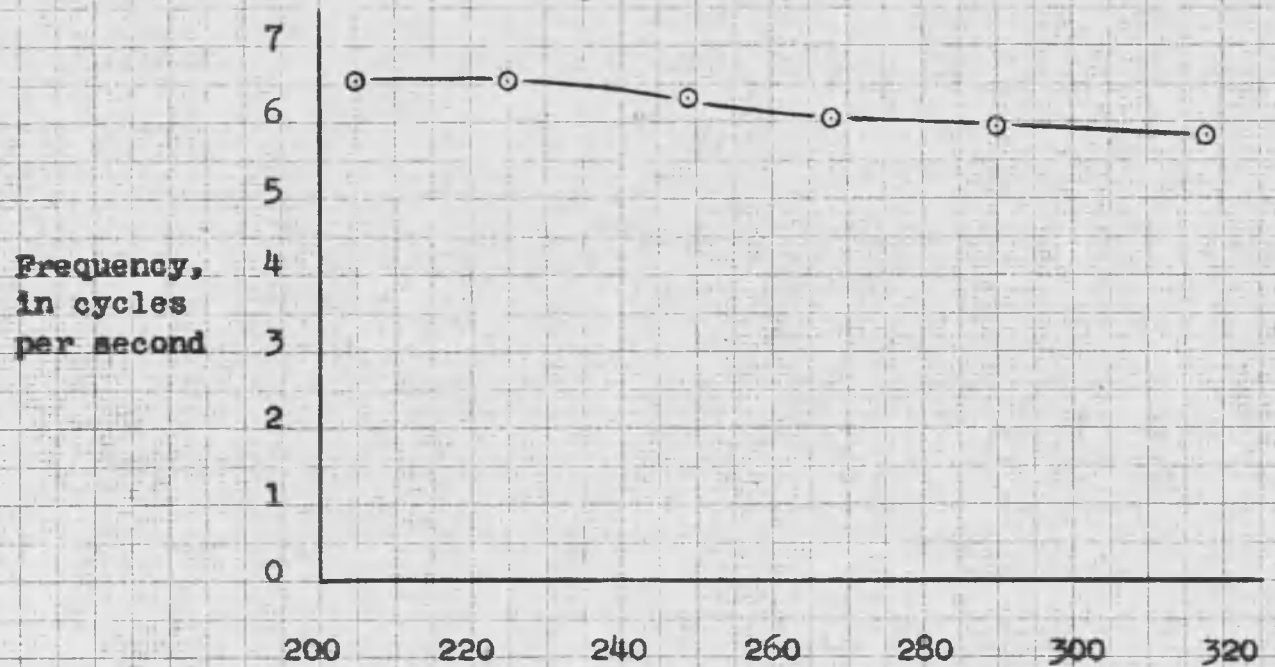

Figure 4.2

Frequency of vertical oscillations of small plenum chamber as a function of power input to fan motor

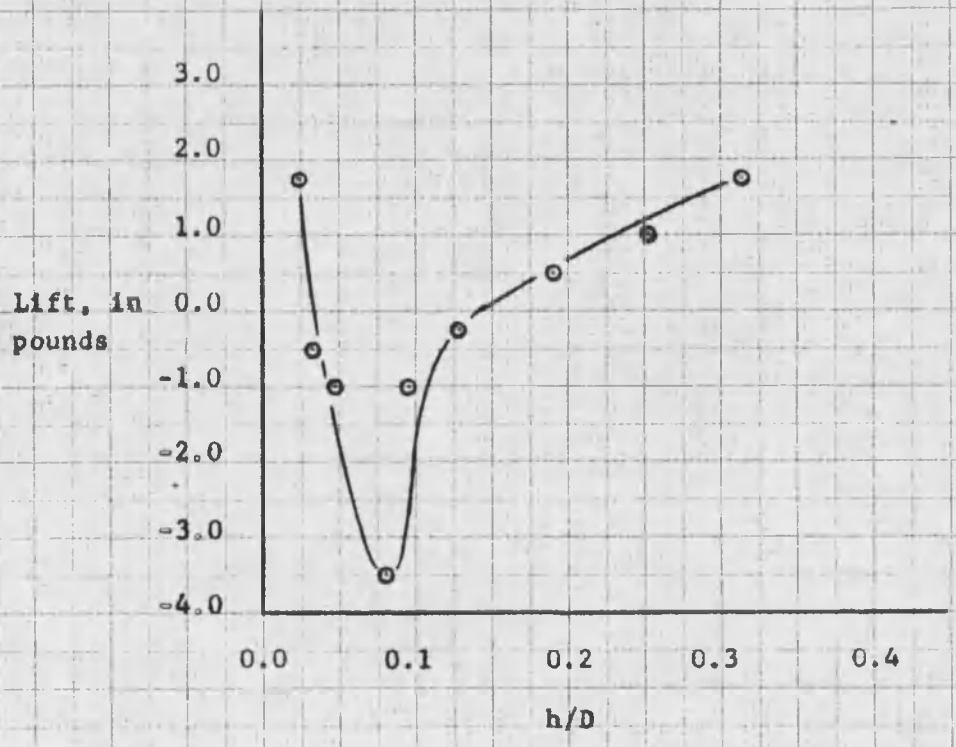

Figure 4.3
Lift produced by small model as a function of h/D

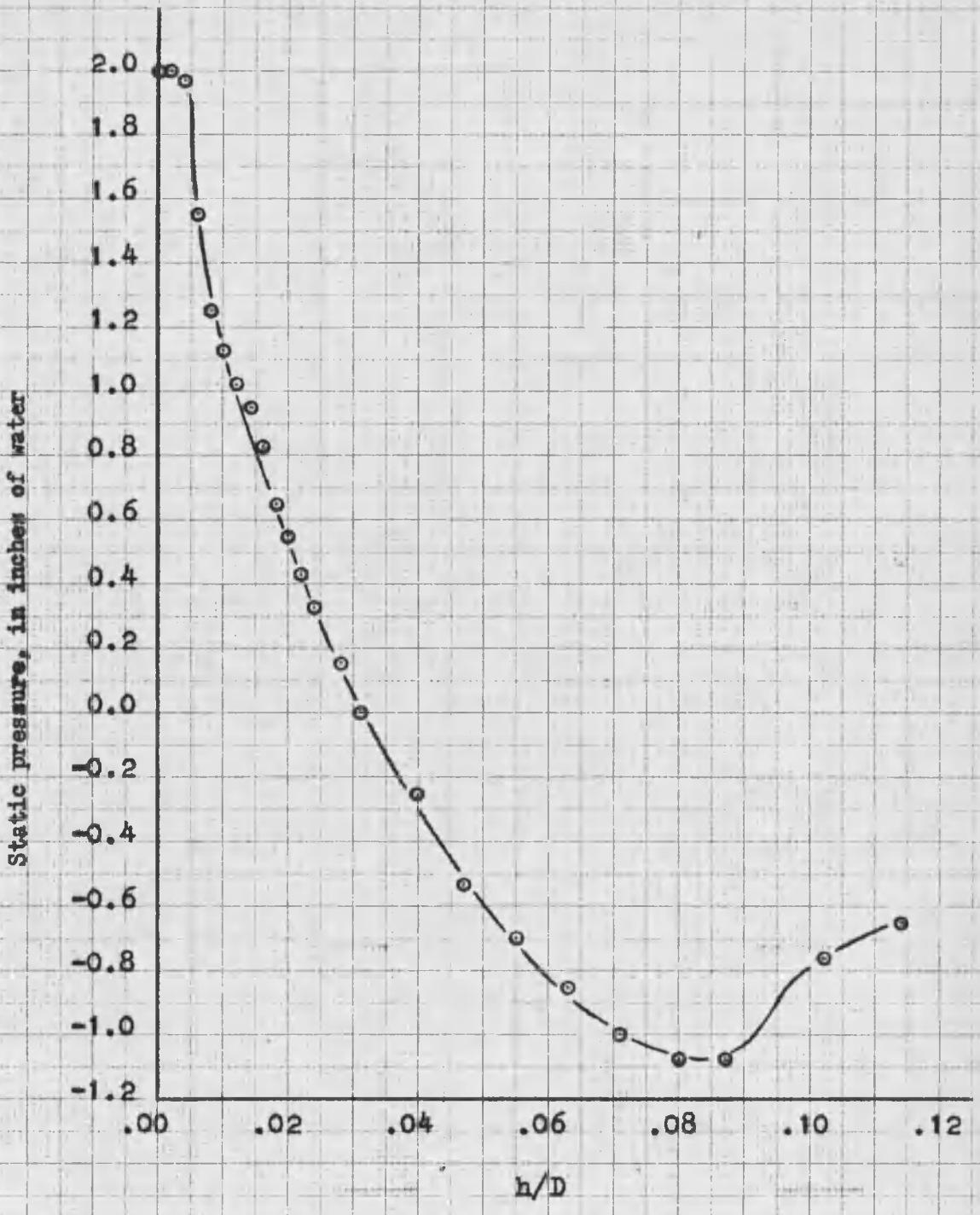

Figure 4.4

Plenum chamber static pressure as a function of h/D

pressure within the plenum chamber is less than the atmospheric pressure on the outside walls of the chamber. This negative lift is believed to be due to high velocity recirculating air within the plenum chamber as noted in Chapter I. At a height of 1.0 inch, h/D = 0.06, the discharge area of the small plenum chamber model is approximately equal to the fan area. According to experiments cited in Chapter I, the plenum chamber should be vented to atmosphere at this height. However, it was observed in the experimental work in this thesis that the maximum negative static pressure occurred at an h/D of about 0.08 which is greater than the h/D where the fan area is equal to the discharge area. Two possible reasons for this difference are that the velocity of the recirculating air in the chamber did not reach its maximum value until the h/D = 0.08 was reached or that a vena-contracta existed at the exit of the plenum chamber which in effect reduced the discharge area. The presence of a vena-contracta has been reported by other authors.[12]

The same negative static pressure was observed in the large plenum chamber model. Figure 4.5 is a photograph of the large plenum chamber model supported by a harness. A multiple tube manometer shows the negative static pressure in the chamber. The tops of the manometer tubes, beginning at the left, were connected to pressure taps 2 through 15 as shown in Figure 2.3, in that order.

Figure 4.5
Negative pressure in large plenum chamber model
(Model supported by harness)

The fifth tube from the right side of the manometer was connected to tap number 1, on the lip of the periphery of the model. The twelfth tube from the left on the manometer was partially closed and gave inaccurate readings. Tubes 15, 17, 18, 19, and 20 were vented to the atmosphere. As illustrated by the photograph, the static pressure within the chamber is below atmospheric and is approximately uniform over the interior surface of the chamber. The pressure tap located on the periphery of the model's lip shows a value between the atmospheric and plenum chamber static pressure. This value indicates that the velocity of the air being discharged is less than the velocity of the recirculating air in the chamber.

4.3 Conclusions -

a) Self-excited vertical oscillations are possible in plenum chamber vehicles.

b) Practical values of h/D for the plenum chamber air cushion vehicle probably will be limited to less than about 0.03. Authors of reference 3 concur with the writer's finding. The self-excited oscillations can occur within this regime of operation.

At higher h/D's a negative lift characteristic can be developed. In the event of a sudden power decrease this condition of negative lift could occur, with serious effects on the vehicle's performance.

These conclusions are essentially qualitative in

nature since all possible pertinent parameters were not controlled due to limitation of the scope of the thesis and time, but they do indicate the general nature of expected behavior.

It is recognized that the work accomplished by this thesis is general in nature and cannot be applied to larger model plenum chambers without further tests being conducted in which all the pertinent parameters are controlled. However, it is felt that this thesis will be of considerable value in planning further tests in this field.

LIST OF REFERENCES

LIST OF REFERENCES

1. R. Stanton Jones, "The Development Of The Saunders-Roe Hovercraft SR-N1", Symposium on Ground Effect Phenomena, Ivy-Curtis Press, Philadelphia, 1959, p. 185.

2. Aeronutronic, "The Role Of The Ground Effect Vehicle In Transportation", Symposium on Ground Effect Phenomena, Ivy-Curtis Press, Philadelphia, 1959, p. 350.

3. National Research Associates, "Test Experience And Comments On Air Cushion Vehicle", Symposium on Ground Effect Phenomena, Ivy-Curtis Press, Philadelphia, 1959, p. 334.

4. H. C. Higgins and L. W. Martin, "Effect of Surface Geometry And Vehicle Motion On Forces Produced By A Ground Pressure Element", Symposium on Ground Effect Phenomena, Ivy-Curtis Press, Philadelphia, 1959, p. 243.

5. Aeronutronic, "State Of The Art Summary, Air-Cushion Vehicles", Aeronutronic Publication Number U-926, June 1960, p. 3-1.

6. K. G. Wernicke, "Performance Testing Of A Five-Foot Air Cushion Model", Symposium on Ground Effect Phenomena, Ivy-Curtis Press, Philadelphia, 1959, p. 364.

7. Ibid., p. 365.

8. National Research Associates, op. cit., p. 334.

9. Wernicke, op. cit., p. 365.

10. Ibid., p. 365.

11. J. P. Den Hartog, Mechanical Vibrations, McGraw-Hill Book Company, Inc., 1940, pp. 328-331.

12. Wernicke, op. cit., p. 364.

APPENDIX

APPENDIX A

SYMBOLS

Symbol	Quantity
c	Viscous damping coefficient
C	Constant of integration
D, d	Diameter of open end of plenum
g	Gravity constant
H	Height above ground at equilibrium hover position
h	Height above ground
k	Specific heat ratio (c_p/c_v)
m	Mass
m_p	Mass of model
P	Pressure
R	Gas constant
S	Planform area (Does not include area of lip)
S_b	Planform area of base of annular jet type vehicle
S_x	Discharge exit area (Perimeter of planform multiplied by height of bottom of plenum chamber above ground)
T	Absolute temperature

t	Time
V	Volume
V_H	Volume of plenum chamber and volume under plan form at equilibrium hover height
v_e	Velocity component perpendicular to discharge area
X	Displacement of plenum chamber from equilibrium hover height
ρ	Density

Subscript

H	Indicates equilibrium hover position
a	Atmospheric pressure
d	Dynamic pressure
x	Indicates a displacement from the equilibrium hover height

A dot above a symbol denotes $\frac{d(\ )}{dt}$; for example

$\dot{m} = \frac{dm}{dt}$

APPENDIX B

DATA

Data for frequency of vertical oscillation of small model (Figure 4.2)

Power to fan motor, in watts Accuracy ± 1 watt	Number of cycles*	Time period for cycles counted, in seconds* Accuracy ± 0.02
205	21.0	3.20
225	21.0	3.20
249	24.0	3.80
268	19.0	3.14
290	38.0	6.40
318	33.0	5.60

*Taken from Sanborn recorder record

Data for lift produced by small model (Figure 4.3)

Height of bottom of model above table, in inches Accuracy $\pm \frac{1}{32}$ inch	Spring scale reading Accuracy $\pm \frac{1}{8}$ pound
3/8	5
1/2	7 1/4
3/4	7 3/4
1 1/4	10 1/4
1 1/2	7 3/4
2	7
3	6 1/4
4	5 3/4
5	5
36	5

Data for static pressure in small model (Figure 4.4)

Pressure readings, in inches of water Accuracy ± 0.012 inch for each leg of manometer		Pressure differential between left leg and right leg of manometer Accuracy ± 0.025 inch	Power to fan motor, in watts Accuracy ± 1 watt	Height of bottom of model from table Accuracy ± 1/64 inch
Left leg	Right leg			
2.450	0.450	2.000	330	0
2.450	0.450	2.000	329	1/32
2.425	0.475	1.975	326	2/32
2.250	0.700	1.550	320	3/32
2.100	0.850	1.250	318	4/32
2.025	0.900	1.125	318	5/32
1.975	0.950	1.025	324	6/32
1.950	1.000	0.950	326	7/32
1.875	1.050	0.825	330	8/32
1.800	1.150	0.650	330	9/32
1.750	1.200	0.550	338	10/32
1.675	1.250	0.425	339	11/32
1.650	1.325	0.325	339	12/32
1.550	1.400	0.150	341	14/32
1.450	1.450	0.000	341	16/32
1.375	1.625	-0.250	345	20/32
1.225	1.750	-0.525	346	24/32
1.150	1.850	-0.700	341	28/32
1.075	1.925	-0.850	340	32/32
1.000	2.000	-1.000	345	36/32
0.925	2.050	-1.075	346	40/32
0.925	2.050	-1.075	348	44/32
1.125	1.875	-0.750	355	52/32
1.150	1.800	-0.650	350	58/32